

1 **N440K variant of SARS-CoV-2 has Higher Infectious Fitness**

2 Dixit Tandel <sup>\*1</sup>, Divya Gupta <sup>\*#</sup>, Vishal Sah <sup>\*#1</sup> and Krishnan Harinivas Harshan <sup>\*#1</sup>

3 <sup>#</sup> These authors contributed equally

4 <sup>\*</sup>Centre for Cellular and Molecular Biology, Hyderabad 500007, India

5 <sup>1</sup>Academy for Scientific and Innovative Research (AcSIR), Ghaziabad-201002, India

6

7 <sup>#</sup>Corresponding author: [hkrishnan@ccmb.res.in](mailto:hkrishnan@ccmb.res.in)

8

9

10

11

12

13

14

15

16

## 17 **SUMMARY**

18 Several variants of SARS-CoV-2 have been emerging across the globe, continuing to  
19 threaten the efforts to end COVID-19 pandemic. Recent data indicate the prevalence of  
20 variants with N440K Spike substitution in several parts of India, which is under the  
21 second wave of the pandemic. Here, we first analyze the prevalence of N440K variants  
22 within the sequences submitted from India and identify a rising trend of its spread  
23 across various clusters. We then compare the replicative fitness and infectivity of a  
24 prototype of this variant with two other previously prevalent strains. The N440K variant  
25 produced ten times higher infectious viral titers than a prevalent A2a strain, and over  
26 1000 folds higher titers than a much less prevalent A3i strain prototype in Caco2 cells.  
27 Similar results were detected in Calu-3 cells as well, confirming the increased potency  
28 of the N440K variant. Interestingly, A3i strain showed the highest viral RNA levels, but  
29 the lowest infectious titers in the culture supernatants, indicating the absence of  
30 correlation between the RNA content and the infectivity of the sample. N440K mutation  
31 has been reported in several viral sequences across India and based on our results, we  
32 predict that the higher infectious titers achieved by N440K variant could possibly lead to  
33 its higher rate of transmission. Availability of more sequencing data in the immediate  
34 future would help understand the potential spread of this variant in more detail.

## 35 **INTRODUCTION**

36 Past one year has witnessed the emergence of several variant strains of the SARS-  
37 CoV-2 (1). Some of them have gained advantage over the original or previously  
38 prevalent strains in spreading across populations and replacing them in due course. Of

39 the several such variants of interest (VoI), a few have been implicated in increased  
40 infectivity and severity. By June 2020, a variant with D614G substitution had become  
41 the predominant strain over the ancestral strains (2). This variant was demonstrated to  
42 have higher fitness (3), (4) over the previously dominant ancestral strains. Later, the UK  
43 variant B.1.1.7 lineage, Brazilian variant P.1 lineage (5) and the South African B.1.351  
44 (6) have emerged as variants of concern (VoC) (1). The newly evolving variants are  
45 expected to have better fitness over their ancestral strains. One prototype of the UK  
46 variants named 20I/501Y.V1 with B.1.1.7 lineage was demonstrated to have higher  
47 replicative fitness over an ancestral D614G strain (7). Comparative studies have also  
48 identified efficient infection and distinct pattern of cytokine induction by these three Vols  
49 (8) indicating that each of these variants establish a unique relationship with the host.

50 In this study, we compared the replicative fitness and infectivity of prototypes of three  
51 SARS-CoV-2 strains. Of these strains, N440K variant with the mutation in Spike is being  
52 increasingly detected in India (<https://data.ccmb.res.in/gear19/>). A3i variant has a  
53 characteristic A97V substitution in RdRP (Nsp12) sequence, while A2a strain has a  
54 D614G substitution in Spike and a P323L substitution in RdRP. N440K variant has  
55 a P323L substitution in RdRP in addition to N440K in Spike. In addition to these, each  
56 of the variant had distinct variations in other sequences. Our studies unambiguously  
57 demonstrate that N440K variant prototype has capacity to generate significantly higher  
58 titers of infectious virus in shorter duration and suggest that this feature could promote  
59 its faster spread among certain populations.

60

## 61 **RESULTS AND DISCUSSION**

### 62 **N440K variant prevalence has been rising in certain clusters in India**

63 We analyzed the GISAID database (9) for the prevalence of variants containing N440K  
64 substitution in Spike. A total of 1555 entries with N440K substitution could be identified  
65 from across the world. Interestingly, India contributed the largest proportion of N440K  
66 variants at 33%, followed by the USA and Germany (Figure 1A). Submissions of  
67 sequences from India contributed to 0.86% of the total submissions (Figure 1B). Of the  
68 submissions from India, 4.9% sequences contained N440K substitution (Figure 1B).  
69 However, when Indian submissions from January 2021 till 24<sup>th</sup> April 2021 were  
70 analyzed, the proportion of N440K substitution significantly went up to 8.82% (Figure  
71 1C). A further breakdown of the recent data indicates a gradual increase in the  
72 representation of this variant with March and April 2021 adding more of this variant than  
73 the previous months (Figure 1D). An increase in the proportion of N440K variant in the  
74 Indian samples is also evident with almost 10% of the sequences submitted in April  
75 2021 carrying this substitution (Figure 1E). Importantly, higher numbers of submissions  
76 with N440K from other parts of the world were seen in the past two months, indicating  
77 its rising spread in such countries (Figure 1F). Significantly, these months also saw  
78 increased submission of sequences from India. Karnataka, Maharashtra, Telangana  
79 and Chhattisgarh together contributed to about 50% of these samples indicating the  
80 geographically localized spread of this variant in India (Figure 2 A and B). Interestingly,  
81 over 99% of the N440K variants were in the background of D641G substitution,  
82 indicating that these variants are in the lineage of A2a strain. Taken together, the data

83 suggests that the proportion of N440K variant has been increasing gradually and  
84 suggesting its improved replicative fitness or increased infectivity.

### 85 **N440K mutant variant makes higher viral titers**

86 Since the proportion of N440K variant has been rising among the sequenced samples  
87 from India, we asked if they have a growth advantage over some of the other strains.  
88 We compared the viral RNA titers of prototypes isolates of three strains from our  
89 repository. The genetic comparison is provided in Figure 3A. The growth of these  
90 viruses in cultured cells was analyzed by measuring the viral RNA titer and infectious  
91 viral titers of the supernatants. RNA titers in the viral culture supernatants are the  
92 default measure of the presence of SARS-CoV-2. Caco2 cells were infected by each of  
93 the three variants at 0.1 MOI. Viral RNA in the supernatants were measured by RT-  
94 qPCR detection of SARS-CoV-2 genes at 24-, 48-, and 72-hours post-infection (hpi). As  
95 indicated by the relative RNA levels (Figure 3 B and C), the A2a strain replicated at  
96 significantly slower rate as compared to the other two strains. Both RdRP and E gene  
97 levels from A2a strain were lower than the other two by over a log. A3i strain had  
98 moderately higher levels of viral RNA than N440K strain until 48 hpi, but both attained  
99 similar RNA levels at 72 hpi. These results indicated that of the three strains, A3i has  
100 higher replicative rate than the other two while A2a replicated at the slowest rate. We  
101 repeated these experiments in another permissive cell line, Calu-3. Here again, A2a  
102 had the lowest RNA titers at 24 hpi, followed by N440K and A3i had the highest (Figure  
103 3 E and F). However, at 48 and 72 hpi, A2a and A3i had almost similar levels of RNA  
104 while N440K had the lowest. These results indicate that A3i has the most competent  
105 replication across multiple cell lines.

106 Next, we measured the infectious viral particles in the supernatants of the infected  
107 Caco2 cells. Surprisingly, N440K variant had the highest infectious viral titers from 24 to  
108 72 hpi while A3i strain had the lowest among the three (Figure 3D). At 72 hpi, N440K  
109 variant achieved infectious titer around  $10^{10}$  PFU/mL, which was three logs (1000 ×)  
110 higher than that of A3i. N440K variant was also produced over 10 times higher numbers  
111 than the A2a prototype. In Calu-3 cells also A3i continued to generate far fewer  
112 infectious virions (Figure 3G). N440K had higher titers at 24 hpi even though this  
113 advantage was not maintained at the later time points. These results clearly  
114 demonstrate that N440K variant prototype is able to generate far more infectious virions  
115 than both A3i and A2a strains and the A3i prototype had the lowest. Our results indicate  
116 that N440K variant has a high potential to become a dominant strain considering its  
117 capacity to produce higher titers of infectious viral particles.

118 N440K mutation has been reported in several clusters in India and our analysis confirms  
119 this. This mutation has been suspected to be responsible for superinfections and quick  
120 spread of the infection in certain pockets. Our studies clearly demonstrate that the  
121 variant carrying this mutation produces large titers of infectious virions more rapidly than  
122 the other two strains tested. More importantly, the ability of N440K variant to generate  
123 about 10 folds more infectious virus particles than the A2a prototype, the strain that has  
124 been in circulation worldwide, assumes significance in the context of its widespread  
125 presence in India and certain other parts of the world. N440K variant is able to generate  
126 larger amounts of viruses in shorter time and hence should be capable of rapid spread  
127 across the population. The ability to generate larger amounts of infectious virus particles  
128 in shorter amount of time could provide it significant advantage over the other

129 competing strains in establishing itself in a large population. Their increasing proportion  
130 in certain clusters validates this observation. Whole genome sequencing data for the  
131 viral strain samples from pan-India would facilitate a better understanding of its  
132 penetration within the Indian population.

133 It is unclear if N440K mutation provides the virus any advantage at the entry or post-  
134 entry stages. Despite sharing the D614G variation, N440K variant differs significantly  
135 from the A2a prototype by having multiple mutations in several Nsps that are shown to  
136 interfere with the host innate immune response (10). A2a strain has been in circulation  
137 across the globe for over several months and is one of the predominant strains (11). On  
138 the other hand, A3i strain that was in circulation during the early periods of the  
139 pandemic has been very limited in circulation. One of the speculated causes for its  
140 disappearance from the population is the A97V substitution in RdRP. The dominant  
141 strains that replaced A3i have a P323L substitution that was reported to have  
142 augmented the polymerase activity, thereby enhancing their replicative fitness resulting  
143 in their dominance (12). However, our studies indicate that this strain is capable of high  
144 levels of replication, but its lower infectious titers could be responsible for its  
145 disappearance from the population. Additional mutations located in Nucleocapsid  
146 (P13L) or in the non-structural proteins could be responsible for their lower infectious  
147 titer. Our studies also underline the fallacy of depending on RT-qPCR and highlight  
148 the importance of measuring the infectious viral titers in such comparative studies.

149

150

## 151 **MATERIALS AND METHODS**

### 152 **Cell culture**

153 Vero (CCL-81) African green monkey kidney epithelial cells, Caco2 colorectal  
154 adenocarcinoma and Calu-3 lung adenocarcinoma cells were cultured in Dulbecco's  
155 Modified Eagle's Medium (DMEM; from Gibco) with Fetal Bovine Serum (FBS; from  
156 Hyclone) and 1× penicillin-streptomycin cocktail (Gibco, 15140-122) at 37°C and 5%  
157 CO<sub>2</sub>. Cells were continuously passaged at 70-80% confluency and mycoplasma  
158 contamination was monitored periodically.

### 159 **SARS-CoV-2 culture, propagation and infection**

160 Three Indian isolates of SARS-CoV-2 strains were used in this study (EPI\_ISL\_539744  
161 (N440K); EPI\_ISL\_458046 (A2a); and EPI\_ISL\_458075 (A3i)). The viruses were  
162 propagated in Vero (CCL-81) cells grown in 1×DMEM deficient in serum and antibiotics.  
163 Caco2 and Calu-3 cells were infected at 0.1 MOI for 2 hours in serum-free conditions  
164 after which the media was replaced with complete media and further incubated until the  
165 time of harvesting. Supernatants collected at the end of time intervals were centrifuged  
166 to remove debris and used for RNA preparation and plaque forming assay.

### 167 **RNA preparation, RT-qPCR and plaque assay**

168 The RNA was isolated using Nucleospin Viral RNA kit (MACHEREY-NAGEL GmbH &  
169 Co. KG) and the SARS-CoV-2 RNA was quantified using a commercial kit (LabGun™  
170 COVID-19 RT-PCR Kit; CV9032B) in Roche LightCycler 480. The Ct values were  
171 normalized against the internal control references provided in the kit.  $\Delta\Delta$ -Ct values were



172 plotted in the graph demonstrating the relative fold changes in the respective samples  
173 against the uninfected control samples. The infectious viral particle numbers in the  
174 supernatant were quantified using plaque-forming unit (PFU/mL) assay in Vero  
175 monolayers. Here, the supernatants were log diluted in 1x serum-free DMEM before  
176 infecting Vero monolayer. 2 hpi the cells were overlaid with agarose: DMEM mix  
177 containing 1% LMA and the plates were incubated for 6 days at 37°C. After the  
178 incubation, the cells were fixed with 4% formaldehyde and stained with crystal violet.  
179 The clear zones were counted and PFU was calculated as PFU/mL.

#### 180 **Infographic analysis on SARS-CoV2 data**

181 The Global initiative on sharing all influenza data (GISAID) database was used for all  
182 infographic analysis used in this study. Firstly, the common mutations in all the three  
183 strains were identified by Venny 2.1.0 (13). Following this, the Venn diagram was made  
184 using Adobe photoshop. For the graph plotting of the infographs, Graphpad Prism was  
185 used. No statistical method was applied to the graphs and no tests to attain significance  
186 was done.

#### 187 **Statistical analysis**

188 All the experiments were performed in a minimum of three independent biological  
189 replicates to generate Mean  $\pm$  SEM which are plotted graphically. For statistical  
190 significance, paired end, two-tailed t-test was performed and represented as *P*-values. \*,  
191 \*\* and \*\*\* indicate *P*-values  $<0.05>0.01$ ,  $<0.01>0.001$  and  $<0.001$  respectively.

192

193 **Institutional ethics clearance**

194 Institutional ethics clearance (IEC-82/2020) was obtained for the patient sample  
195 processing for virus culture.

196 **Institutional biosafety**

197 Institutional biosafety clearance was obtained for the experiments pertaining to SARS-  
198 CoV-2.

199 **Acknowledgements**

200 We thank the NGS team at CCMB for providing the sequences the SARS-CoV-2 strains  
201 used in this study. Several volunteers at the Centre for Cellular and Molecular Biology,  
202 who were part of COVID-19 testing, helped us gain access to the potential patient  
203 samples for virus culturing. Special thanks to Amit Kumar and Mohan Singh Moodu for  
204 their help with the logistics.

205 **Funding**

206 This study was funded by the internal funds of CSIR-CCMB.

207 **Author Contributions**

208 D.K., D.G., and K.H.H. conceptualized the study. D.K. set up the infections and  
209 performed RT-qPCR. D.G performed plaque forming assays. V.S performed the various  
210 comparative analyses of the viral genomes. K.H.H. wrote the manuscript with the  
211 assistance from the other authors.

212

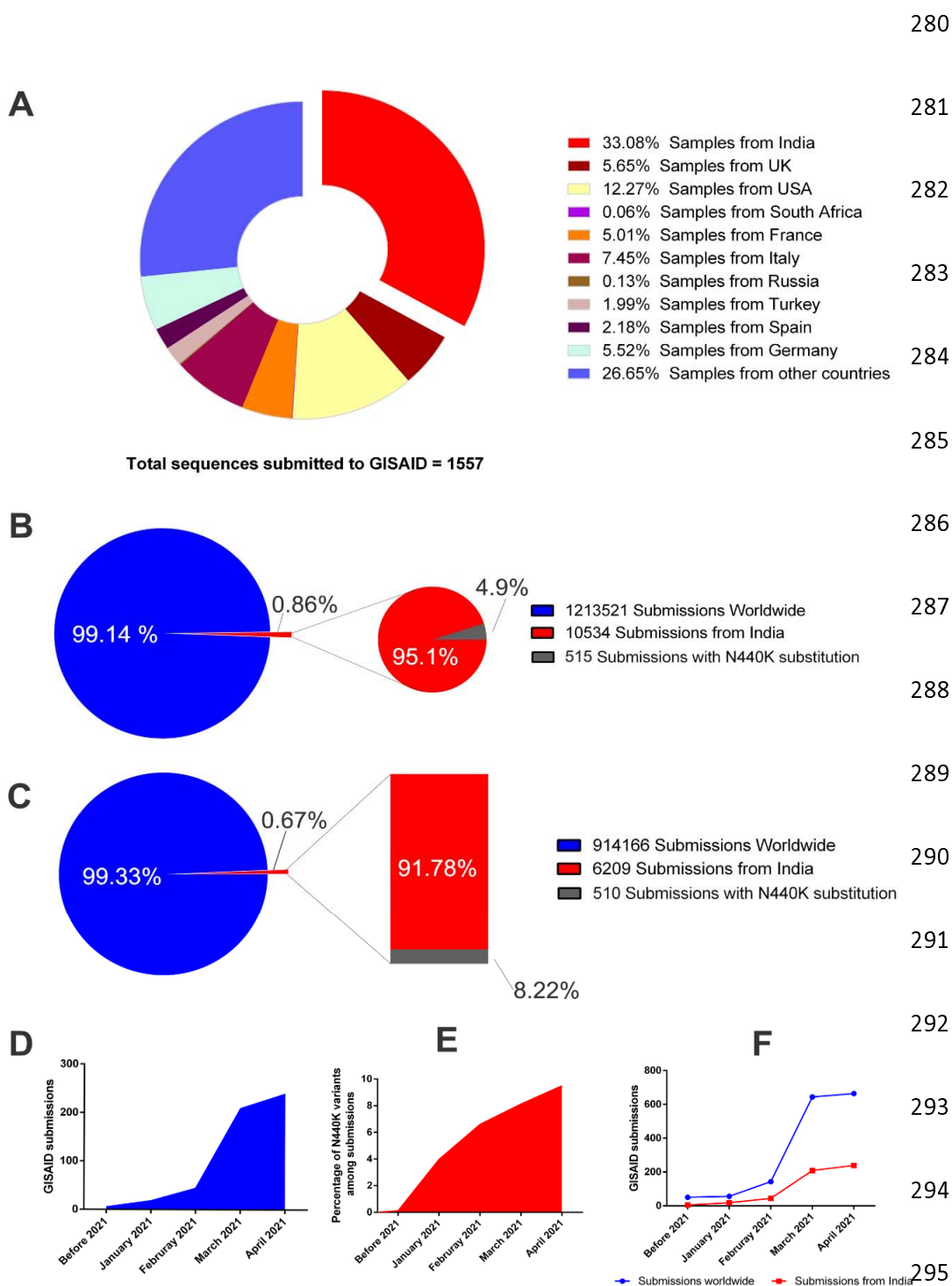
213 **REFERENCES**

- 214 1. Science Brief: Emerging SARS-CoV-2 Variants | CDC.
- 215 2. Yurkovetskiy L, Wang X, Pascal KE, Tomkins-Tinch C, Nyalile TP, Wang Y, Baum  
216 A, Diehl WE, Dauphin A, Carbone C, Veinotte K, Egri SB, Schaffner SF, Lemieux  
217 JE, Munro JB, Rafique A, Barve A, Sabeti PC, Kyratsous CA, Dudkina N V., Shen  
218 K, Luban J. 2020. Structural and Functional Analysis of the D614G SARS-CoV-2  
219 Spike Protein Variant. *Cell* 183:739-751.e8.
- 220 3. Plante JA, Liu Y, Liu J, Xia H, Johnson BA, Lokugamage KG, Zhang X, Muruato  
221 AE, Zou J, Fontes-Garfias CR, Mirchandani D, Scharton D, Bilello JP, Ku Z, An Z,  
222 Kalveram B, Freiberg AN, Menachery VD, Xie X, Plante KS, Weaver SC, Shi PY.  
223 2021. Spike mutation D614G alters SARS-CoV-2 fitness. *Nature* 592:116–121.
- 224 4. Korber B, Fischer WM, Gnanakaran S, Yoon H, Theiler J, Abfalterer W,  
225 Hengartner N, Giorgi EE, Bhattacharya T, Foley B, Hastie KM, Parker MD,  
226 Partridge DG, Evans CM, Freeman TM, de Silva TI, Angyal A, Brown RL,  
227 Carrilero L, Green LR, Groves DC, Johnson KJ, Keeley AJ, Lindsey BB, Parsons  
228 PJ, Raza M, Rowland-Jones S, Smith N, Tucker RM, Wang D, Wyles MD,  
229 McDanal C, Perez LG, Tang H, Moon-Walker A, Whelan SP, LaBranche CC,  
230 Sapphire EO, Montefiori DC. 2020. Tracking Changes in SARS-CoV-2 Spike:  
231 Evidence that D614G Increases Infectivity of the COVID-19 Virus. *Cell* 182:812-  
232 827.e19.
- 233 5. Faria NR, Mellan TA, Whittaker C, Claro IM, Candido D da S, Mishra S, Crispim  
234 MAE, Sales FCS, Hawryluk I, McCrone JT, Hulswit RJG, Franco LAM, Ramundo

- 235 MS, de Jesus JG, Andrade PS, Coletti TM, Ferreira GM, Silva CAM, Manuli ER,  
236 Pereira RHM, Peixoto PS, Kraemer MUG, Gaburo N, Camilo C da C,  
237 Hoeltgebaum H, Souza WM, Rocha EC, de Souza LM, de Pinho MC, Araujo LJT,  
238 Malta FS V., de Lima AB, Silva J do P, Zauli DAG, Ferreira AC de S,  
239 Schnekenberg RP, Laydon DJ, Walker PGT, Schlüter HM, dos Santos ALP, Vidal  
240 MS, Del Caro VS, Filho RMF, dos Santos HM, Aguiar RS, Proença-Modena JL,  
241 Nelson B, Hay JA, Monod M, Miscouridou X, Coupland H, Sonabend R, Vollmer  
242 M, Gandy A, Prete CA, Nascimento VH, Suchard MA, Bowden TA, Pond SLK, Wu  
243 C-H, Ratmann O, Ferguson NM, Dye C, Loman NJ, Lemey P, Rambaut A, Fraiji  
244 NA, Carvalho M do PSS, Pybus OG, Flaxman S, Bhatt S, Sabino EC. 2021.  
245 Genomics and epidemiology of the P.1 SARS-CoV-2 lineage in Manaus, Brazil.  
246 Science (80- ) eabh2644.
- 247 6. Tegally H, Wilkinson E, Giovanetti M, Iranzadeh A, Fonseca V, Giandhari J,  
248 Doolabh D, Pillay S, San EJ, Msomi N, Mlisana K, von Gottberg A, Walaza S,  
249 Allam M, Ismail A, Mohale T, Glass AJ, Engelbrecht S, van Zyl G, Preiser W,  
250 Petruccione F, Sigal A, Hardie D, Marais G, Hsiao M, Korsman S, Davies MA,  
251 Tyers L, Mudau I, York D, Maslo C, Goedhals D, Abrahams S, Laguda-Akingba  
252 O, Alisoltani-Dehkordi A, Godzik A, Wibmer CK, Sewell BT, Lourenço J, Alcantara  
253 LCJ, Kosakovsky Pond SL, Weaver S, Martin D, Lessells RJ, Bhiman JN,  
254 Williamson C, de Oliveira T. 2020. Emergence and rapid spread of a new severe  
255 acute respiratory syndrome-related coronavirus 2 (SARS-CoV-2) lineage with  
256 multiple spike mutations in South Africa. medRxiv. medRxiv.
- 257 7. Touret F, Luciani L, Baronti C, Cochin M, Driouich J-S, Gilles M, Thirion L,

- 258 Nougairède A, De Lamballerie X. 1207. Replicative fitness SARS-CoV-2  
259 20I/501Y.V1 variant in a human reconstituted 1 bronchial epithelium  
260 <https://doi.org/10.1101/2021.03.22.436427>.
- 261 8. Abdelnabi R, Boudewijns R, Foo CS, Seldeslachts L, Zhang X, Delang L, Maes P,  
262 F Kaptein SJ, Vande Velde G, Neyts J, Dallmeier K. 2021. Comparative infectivity  
263 and pathogenesis of emerging SARS-CoV-2 variants in Syrian 1 hamsters 2 3 4.  
264 bioRxiv 2021.02.26.433062.
- 265 9. Shu Y, McCauley J. 2017. GISAID: Global initiative on sharing all influenza data –  
266 from vision to reality. Eurosurveillance.
- 267 10. Xia H, Cao Z, Xie X, Zhang X, Chen JYC, Wang H, Menachery VD, Rajsbaum R,  
268 Shi PY. 2020. Evasion of Type I Interferon by SARS-CoV-2. Cell Rep 33.
- 269 11. Baric RS. 2020. Emergence of a Highly Fit SARS-CoV-2 Variant. N Engl J Med  
270 383:2684–2686.
- 271 12. Pachetti M, Marini B, Benedetti F, Giudici F, Mauro E, Storici P, Masciovecchio C,  
272 Angeletti S, Ciccozzi M, Gallo RC, Zella D, Ippodrino R. 2020. Emerging SARS-  
273 CoV-2 mutation hot spots include a novel RNA-dependent-RNA polymerase  
274 variant. J Transl Med 18:179.
- 275 13. -Venny-. Venn Diagrams for comparing lists. By Juan Carlos Oliveros.  
276  
277  
278

279 Figure 1



296

297 **Figure 1. Analysis of the prevalence of N440K Spike variant of SARS-CoV-2.** (A)

298 demonstrates its prevalence across the world based on the sequences submitted to

299 GISAID. (B) compares the proportion of N440K variant sequences submitted from India.

300 The blue circle shows the submissions from across the world and the red circle shows

301 the sequences from India. (C) Comparison as in (B), but the data points are selected

302 from January, 2021 till 24<sup>th</sup> April, 2021. (D) shows the increasing numbers of N440K

303 carrying sequences from India since the beginning of 2021 and (E) its proportion in the

304 total sequences submitted. (F) demonstrates the number of sequences containing

305 N440K substitution from India and the rest of the world.

306

307

308

309

310

311

312

313

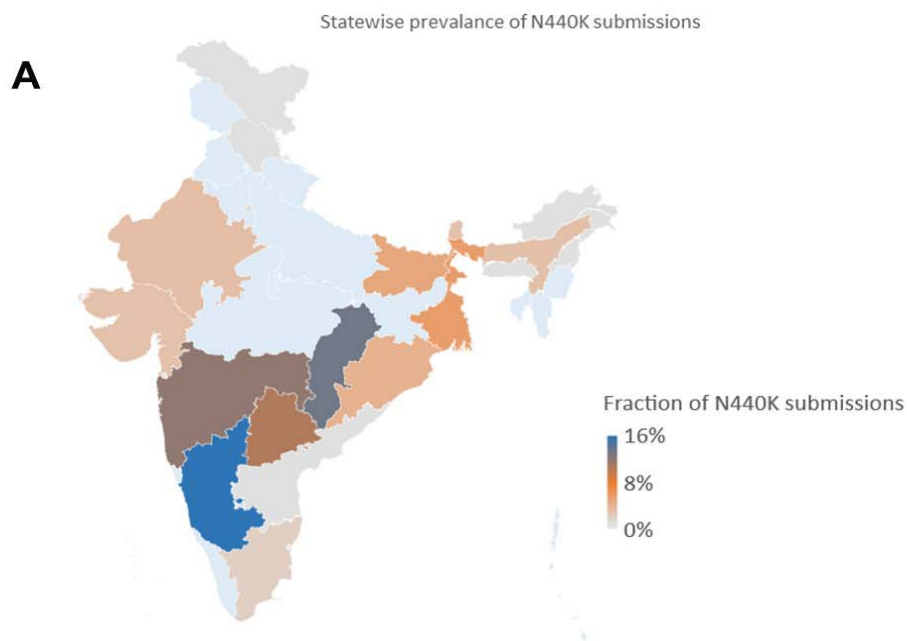
314

315

316

317 **Figure 2**

318



**B**

State	No. of sequences submitted to GISAID from Jan 2021	No. of sequences with N440K substitution
Andaman and Nicobar Islands	1	0
Assam	32	1
Bihar	41	2
Chhattisgarh	320	42
Gujrat	293	9
Chandigarh	21	0
Karnataka	339	54
Telangana	773	81
Maharashtra	772	91
Odisha	266	11
Rajasthan	31	1
Goa	5	0
Haryana	43	0
Himanchal Pradesh	34	0
Jammu and Kashmir	21	0
Jharkhand	67	0
Kerala	106	0
Madhya Pradesh	19	0
Manipur	22	0
Mizoram	63	0
Punjab	67	0
Sikkim	34	1
Tamil Nadu	49	1
Tripura	19	0
Uttar Pradesh	22	0
West Bengal	1176	66
Uttarakhand	22	0
Other regions	1551	150
<b>Total</b>	<b>6209</b>	<b>510</b>



319 **Figure 2. Geographic distribution of N440K variant across India as of April 24,**  
320 **2021.** Whole genome sequences available from GISAID were analyzed based on their  
321 sample origin. (A) demonstrates the heatmap of the distribution. The highest intensity is  
322 represented by blue while the lowest by grey. (B) Table detailing the number of  
323 sequences originated from the states and the number o N440K variants reported from  
324 the corresponding states.

325

326

327

328

329

330

331

332

333

334

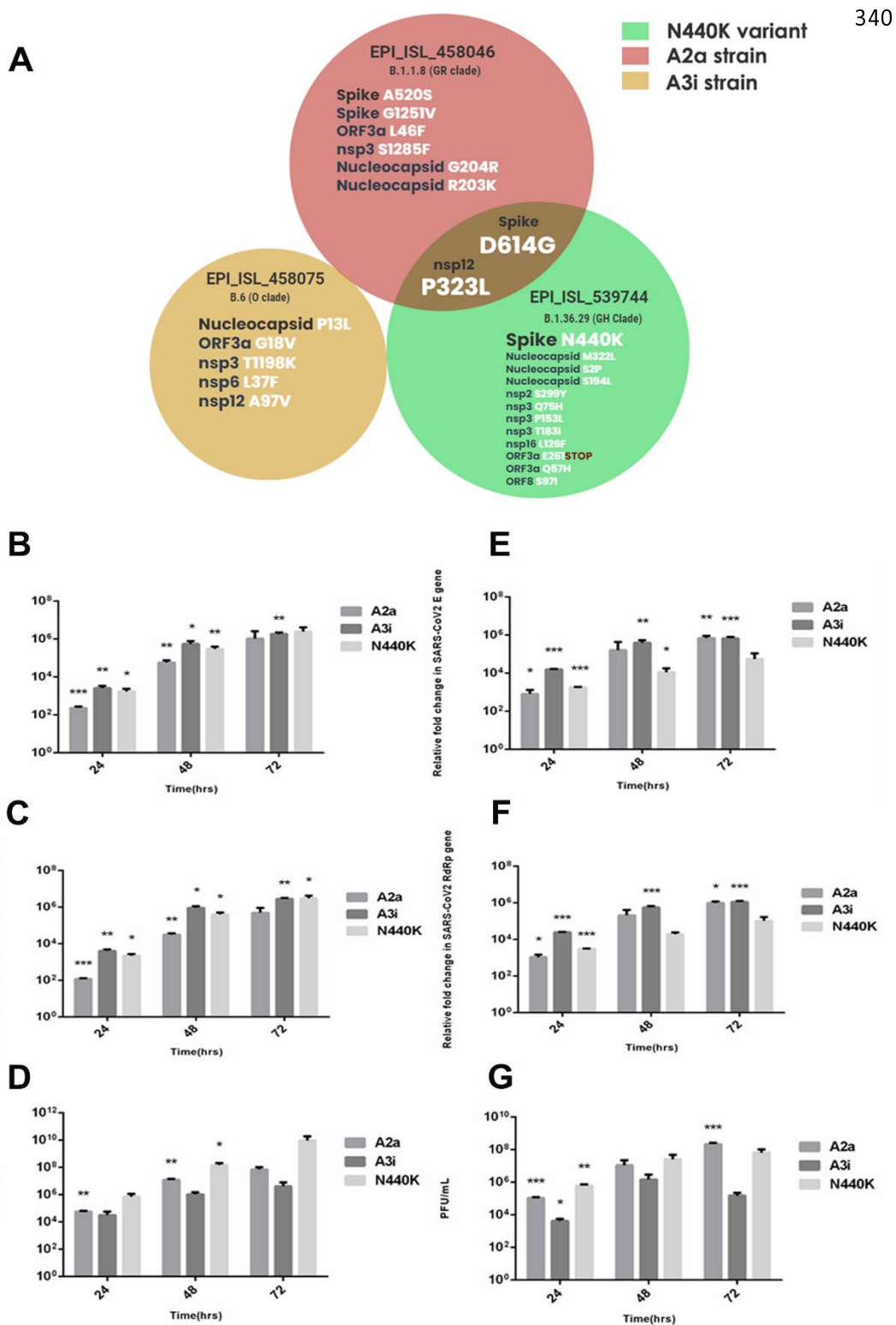
335

336

337

338

339 Figure 3



341 **Figure 3. Analysis of the replicative fitness and infectious viral particle generation**  
342 **for three variants used in this study.** (A) Comparison of genetic diversity among the  
343 three variants. (B-D) Caco2 cells were infected with 0.1 MOI of three viral variants for  
344 24-, 48- and 72 hours. At the end of these time intervals, supernatants were collected  
345 and processed. (D) represents the absolute plaque units per mL of the supernatant  
346 collected at the respective time point. (E-G) Similar experiments and analyses  
347 performed in Calu-3 cells.

348

349

350

351

352

353

354

355

356

357

358

359

360

361

362

363

364

365

366